^{19}Ne level structure for explosive nucleosynthesis

M. R. Hall,[1,2,*] D. W. Bardayan,[1] T. Baugher,[3] A. Lepailleur,[3] S. D. Pain,[2] A. Ratkiewicz,[3] S. Ahn,[4] J. M. Allen,[1] J. T. Anderson,[5] A. D. Ayangeakaa,[5] J. C. Blackmon,[6] S. Burcher,[7] M. P. Carpenter,[5] S. M. Cha,[8] K. Y. Chae,[8] K. A. Chipps,[2,7] J. A. Cizewski,[3] M. Febbraro,[2] O. Hall,[1,9] J. Hu,[1] C. L. Jiang,[5] K. L. Jones,[7] E. J. Lee,[8] P. D. O'Malley,[1] S. Ota,[10] B. C. Rasco,[6] D. Santiago-Gonzalez,[6] D. Seweryniak,[5] H. Sims,[3,9] K. Smith,[7] W. P. Tan,[1] P. Thompson,[2,7] C. Thornsberry,[7] R. L. Varner,[2] D. Walter,[3] G. L. Wilson,[6,11] and S. Zhu[5,12]

[1]*Department of Physics, University of Notre Dame, Notre Dame, Indiana 46556, USA*
[2]*Physics Division, Oak Ridge National Laboratory, Oak Ridge, Tennessee 37831, USA*
[3]*Department of Physics and Astronomy, Rutgers University, New Brunswick, New Jersey 08903, USA*
[4]*National Superconducting Cyclotron Laboratory, Michigan State University, East Lansing, Michigan 48824, USA*
[5]*Physics Division, Argonne National Laboratory, Argonne, Illinois 60439, USA*
[6]*Department of Physics and Astronomy, Louisiana State University, Baton Rouge, Louisiana 70803, USA*
[7]*Department of Physics and Astronomy, University of Tennessee, Knoxville, Tennessee 37996, USA*
[8]*Department of Physics, Sungkyunkwan University, Suwon 16419, South Korea*
[9]*Department of Physics, University of Surrey, Guildford, Surrey GU2 7XH, United Kingdom*
[10]*Physics Division, Lawrence Livermore National Laboratory, Livermore, California 94551, USA*
[11]*Department of Physics and Applied Physics, University of Massachusetts Lowell, Lowell, Massachusetts 01854, USA*
[12]*National Nuclear Data Center, Brookhaven National Laboratory, Upton, New York 11973, USA*

(Received 26 May 2020; revised 7 August 2020; accepted 16 September 2020; published 6 October 2020)

Background: ^{19}Ne is an important isotope in nuclear astrophysics due to its role in both the ^{18}F$(p,\alpha)^{15}$O and ^{15}O$(\alpha,\gamma)^{19}$Ne reactions in novae and Type I x-ray bursts, respectively. The energy levels of ^{19}Ne near the α and proton thresholds ($S_\alpha = 3529$ keV, $S_p = 6410$ keV) correspond to resonances in both of these reactions. Previous measurements to study the structure of ^{19}Ne have focused on both regions in an effort to constrain these reaction rates.

Purpose: Discrepancies in the energies, spins, and parities for levels in ^{19}Ne from previous measurements contribute to the reaction-rate uncertainties. Gamma rays from the depopulation of excited states in ^{19}Ne were measured to reduce the level-energy uncertainties and inconsistencies in previous spin-parity assignments.

Methods: The ^{19}F$(^3$He$, t)^{19}$Ne reaction was used to elucidate the structure of ^{19}Ne levels up to $E_x = 6.9$ MeV. The reaction products were measured using Gammasphere ORRUBA: Dual Detectors for Experimental Structure Studies—a coupling of the Oak Ridge Rutgers University Barrel Array and Gammasphere at Argonne National Laboratory. Tritons produced in the reaction were measured in coincidence with γ rays from the deexcitation of ^{19}Ne energy levels.

Results: Previously unobserved transitions allowed for discrepancies in the resonance properties relevant to these two reactions to be resolved. In total, 41 transitions from 21 energy levels were measured in ^{19}Ne, with 21 of those transitions being previously unobserved. Of particular importance, transitions from two $3/2^+$ states with energies of 6423(3) and 6441(3) keV, crucial for accurate estimations of the ^{18}F$(p,\alpha)^{15}$O reaction rate, were found.

Conclusions: Energies and spin-parities of important energy levels near the proton and α thresholds were measured and some of the discrepancies in previous measurements were resolved. Measurement of the two near-threshold $3/2^+$ states reduced the calculated upper limit of the ^{18}F$(p,\alpha)^{15}$O reaction rate by factors of 1.5–17 in the nova temperature range.

DOI: 10.1103/PhysRevC.102.045802

I. INTRODUCTION

Knowledge of the nuclear structure of ^{19}Ne above the α and proton thresholds is important for accurate estimations of the nucleosynthesis occurring in Type I x-ray bursts and novae. In Type I x-ray bursts, the energy levels near the α threshold ($S_\alpha = 3529$ keV) correspond to resonances in the ^{15}O$(\alpha,\gamma)^{19}$Ne reaction, which is important for breakout from the hot carbon-nitrogen-oxygen (CNO) cycles into the rp process [1,2]. The levels above the proton threshold ($S_p = 6410$ keV), however, are interesting for nova explosion nucleosynthesis because they determine the rate at which ^{18}F is destroyed by proton-induced reactions [3]. The 511-keV γ-ray line and lower-energy continuum generated when ^{18}F β^+ decays is a leading candidate for observation with space-based

*mhall12@alumni.nd.edu

γ-ray observatories [4]. An accurate estimation of the abundance of ^{18}F nuclei remaining to decay after the explosion is necessary to determine at what distances γ rays from novae can be detected and what γ-ray telescope sensitivities are required.

Since no detected nuclear γ rays have been directly attributed to a specific nova explosion, much of the effort over the past two decades has focused on reducing these proton-capture reaction-rate uncertainties important for nova nucleosynthesis [3,5–9]. Of the two reactions that destroy ^{18}F, the $^{18}\mathrm{F}(p,\alpha)^{15}\mathrm{O}$ reaction is approximately 1000 times faster than $^{18}\mathrm{F}(p,\gamma)^{19}\mathrm{Ne}$ [10] and therefore has garnered the most attention in recent studies. The energy levels in ^{19}Ne that have the most influence on the $^{18}\mathrm{F}(p,\alpha)^{15}\mathrm{O}$ reaction rate are those with spin-parities of $J^\pi = 1/2^+$ or $3/2^+$ because they correspond to s-wave ($\ell = 0$) resonances. Therefore, accurately measuring the spin-parities and energies of these levels is imperative to reducing the reaction-rate uncertainties.

A $3/2^+$ state in ^{19}Ne has previously been measured by Ref. [11] with an excitation energy of 7075.7 ± 1.6 keV, which corresponds to a resonance energy of $E_r = 665$ keV. This resonance is broad, meaning it will influence the proton capture rate over a wide range of temperatures. Other $3/2^+$ energy levels in ^{19}Ne near the proton threshold will also interfere with the wave function of this state, increasing the uncertainty in the rate. Measurements of the near-threshold-level properties are difficult, but some information on the ^{19}Ne levels can be inferred from studies of its stable mirror nucleus, ^{19}F. There are two known $3/2^+$ ^{19}F states in the appropriate energy range ($E_x = 6497$ and 6527 keV), which has led to many attempts to determine the analog energies in ^{19}Ne [3,5,7,12].

Utku *et al.* [3] was the first to study some of these near-threshold levels by measuring the $^{19}\mathrm{F}(^3\mathrm{He},t)^{19}\mathrm{Ne}$ reaction with the Princeton quadrupole-dipole-dipole-dipole (Q3D) spectrograph. A doublet of energy levels near the proton threshold were observed with energies of 6419 ± 6 and 6449 ± 6 keV. These levels were postulated to have spin-parities of $3/2^+$ based solely on the level structure of the mirror nucleus. Subsequent measurements of $^{18}\mathrm{F}(d,p)^{19}\mathrm{F}$ were performed to study neutron single-particle states in ^{19}F [13,14] and observed a strong $3/2^+$ level population in ^{19}F. Proton single-particle states in ^{19}Ne were also probed using the $^{18}\mathrm{F}(d,n)^{19}\mathrm{Ne}$ reaction by Adekola *et al.* [5,15,16], indicating the 6419-keV state from Ref. [3] was $J^\pi = 3/2^-$. This spin-parity was determined via analysis of neutron angular distributions, reconstructed from the detection of correlated α particles and ^{15}O nuclei from the breakup of ^{19}Ne. Also observed was a new subthreshold resonance at $E_r = -121$ keV ($J^\pi = 1/2^+$ or $3/2^+$). No above-threshold $3/2^+$ states were observed, leading to upper limits on the proton width and spectroscopic factor for a $3/2^+$ state at $E_x = 6449$ keV of $\Gamma_p \leqslant 2.35 \times 10^{-15}$ keV and $S_p \leqslant 0.028$, respectively. The $E_r = -121$ keV state was confirmed to be $J^\pi = 1/2^+$ by Bardayan *et al.* [8].

Additional studies of ^{19}Ne using the $^{19}\mathrm{F}(^3\mathrm{He},t)^{19}\mathrm{Ne}$ reaction were performed by Laird *et al.* and Parikh *et al.* [7,12]. Triton spectra measured with the Maier-Leibnitz-Laboratorium Q3D indicated the possibility that the above-threshold doublet observed by Ref. [3] was actually a triplet of states with energies $E_x = 6416$, 6440, and 6459 keV. Crucially, it was found that the angular distributions of these states were inconsistent with a spin-parity of $3/2^+$, which would greatly reduce their importance in the $^{18}\mathrm{F}(p,\alpha)^{15}\mathrm{O}$ reaction rate.

Most recently, a study of the $^{19}\mathrm{F}(^3\mathrm{He},t)^{19}\mathrm{Ne}$ reaction was performed by Kahl *et al.* [17] at the Research Center for Nuclear Physics (RCNP) using the "Grand Raiden" spectrometer. This study specifically searched for s-wave resonances in $^{18}\mathrm{F}(p,\alpha)^{15}\mathrm{O}$. A state at $E_x = 6130$ keV was observed, and it was speculated to be either $J^\pi = 1/2^+$ or $3/2^+$. Since the only $1/2^+$ state in ^{19}F in this region was accounted for by Ref. [8] and the energy is likely too low to be the mirror of the 6497- or 6527-keV ^{19}F states, the nature of this state is still uncertain.

To address some of the outstanding questions regarding the level structure of ^{19}Ne, the $^{19}\mathrm{F}(^3\mathrm{He},t)^{19}\mathrm{Ne}$ reaction was studied by detecting both the reaction tritons and γ rays emitted from the deexcitation of the populated ^{19}Ne excited states. This is the first time that γ rays from states above the proton threshold have been measured in ^{19}Ne. The results of this work were first presented in Hall *et al.* [9], and this follow-up paper further expands on the analysis details and results.

II. EXPERIMENT

A 30 MeV beam of ^{3}He with an average intensity of 2.5 pnA was delivered at Argonne National Laboratory by the ATLAS accelerator onto a 938 μg/cm^2 CaF_2 target to induce the $^{19}\mathrm{F}(^3\mathrm{He},t)^{19}\mathrm{Ne}$ reaction. The target was mounted in the center of Gammasphere ORRUBA: Dual Detectors for Experimental Structure Studies (GODDESS) [18,19] which is a coupling of the Oak Ridge Rutgers University Barrel Array (ORRUBA) [20], a $\approx 4\pi$ array of position-sensitive silicon detectors, and Gammasphere, an array of Compton-suppressed high-purity germanium detectors [21]. Tritons from the reaction were detected in ORRUBA in coincidence with γ rays from the deexcitation of the energy levels populated in ^{19}Ne.

The ORRUBA array consists of Micron BB10-Super X3ΔE-E telescopes in a barrel configuration, each having thicknesses of 65 and 1000 μm, respectively. For the $^{19}\mathrm{F}(^3\mathrm{He},t)^{19}\mathrm{Ne}$ experiment, only the telescopes in the downstream half of the barrel were used. The downstream endcap of ORRUBA was augmented with Micron QQQ5 telescopes having thicknesses of 100 and 1000 μm for the ΔE and E detector, respectively. These detectors were also shielded from elastically scattered ^{3}He by a 0.5-mm-thick aluminum plate, which was thin enough to allow transmission of the reaction tritons.

A particle identification (PID) spectrum taken at $\theta_{\mathrm{Lab}} = 20^\circ$ in the QQQ5 telescopes can be found in Fig. 1. The PID spectrum allowed events from the $(^3\mathrm{He},t)$ reaction to be separated from the ejectiles of other unwanted reaction channels. The total detected energy of the tritons was then used to produce a ^{19}Ne excitation energy (E_x) spectrum from the reaction kinematics, which can be found in the upper panel of Fig. 2. For comparison, the lower panel in Fig. 2 shows the locations of previously measured ^{19}Ne excited states as

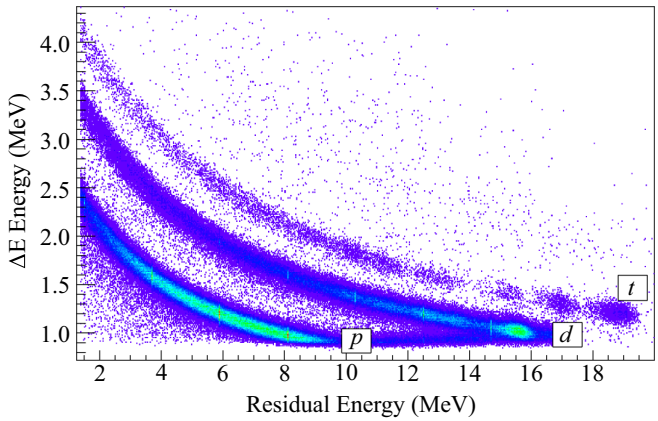

FIG. 1. Particle identification spectrum from the QQQ5 detectors, detected at $\theta_{\text{Lab}} = 20°$. The elastically scattered ^{3}He beam was completely blocked by the aluminum blocker and not detected. Tritons from the reaction of interest are clearly separated from the protons and deuterons produced by the other reactions on the target. Adapted from Ref. [22].

reported in Ref. [23]. Additional details regarding the experimental setup and analysis can be found in Refs. [9,24,25].

Calibration of each Gammasphere detector was necessary to search for γ rays from ^{19}Ne in a summed Gammasphere spectrum and to precisely determine their energies. Three sources were used in the calibration: ^{152}Eu, which provided γ rays below 1500 keV, ^{56}Co, which decays to ^{56}Fe producing three strong γ rays between 800 and 2600 keV, and $^{238}\text{Pu} + {}^{13}\text{C}$, which produces a high-energy γ ray from ^{16}O via $^{13}\text{C}(\alpha, n)\,^{16}\text{O}$ at 6128 keV. The third source crucially allowed for an accurate calibration at high energies, near where transitions from the above-threshold states in ^{19}Ne were expected. A linear calibration was used for each detector, which provided the best energy reproduction for known γ rays and the smallest uncertainty on the fit parameters.

Doppler correction

The Doppler correction of reaction photons was key in the search for γ-ray transitions from short-lived ^{19}Ne states. The ^{19}Ne recoils produced in the reaction stopped in the target, and the stopping time was estimated using the semi-empirical Stopping Range of Ions in Matter (SRIM) program to be roughly 665 fs, assuming an initial average kinetic energy of 0.8 MeV. Therefore, the γ rays produced from ^{19}Ne excited states with short lifetimes ($\tau \lesssim 1$ ps) needed a Doppler correction.

Of the well-known ^{19}Ne states below $E_x = 5$ MeV, only two have lifetimes long enough to allow the ^{19}Ne recoils to stop in the target before decaying: $E_x = 1508$ keV ($\tau = 1.7(3)$ ps [26]) and $E_x = 4634$ keV ($\tau > 1$ ps [26]). It was thus assumed that all other γ rays required a correction to be properly observed, and the following equation was applied to the Gammasphere spectra:

$$E_{\gamma,0} = E_\gamma \left(\frac{\sqrt{1-\beta^2}}{1-\beta\cos\theta_{\text{Doppler}}} \right)^{-1}, \tag{1}$$

where $E_{\gamma,0}$ is the original γ-ray energy, E_γ is the detected γ-ray energy, β is the velocity of the ^{19}Ne recoil given by v/c, and θ_{Doppler} is the angle between the ^{19}Ne recoil direction and the emitted γ ray. The ^{19}Ne recoil velocity and Doppler angle were calculated for each coincident triton and γ ray using the detected triton angle. The detected triton energy had a minimal effect on the calculated ^{19}Ne velocity.

To evaluate the Doppler correction, $\beta = \kappa\beta_{\text{calc}}$ was used, where β_{calc} is the maximum value of β calculated using the reaction kinematics, and κ is the fraction of β_{calc} applied in the Doppler equation. Figure 3 shows the effect that gradually increasing the value of κ has on the 4140-keV transition from

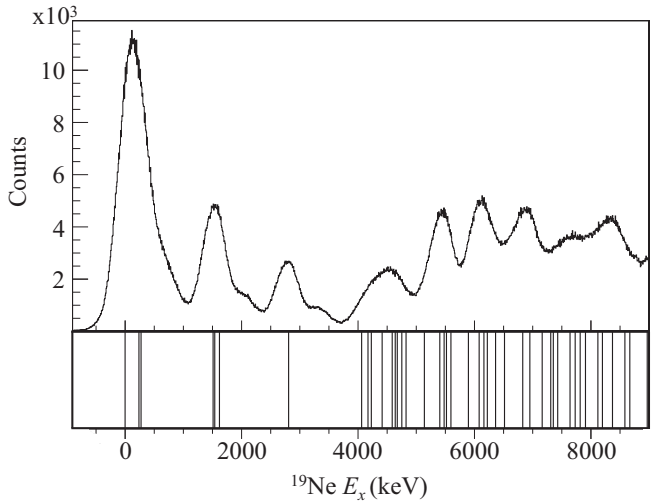

FIG. 2. ^{19}Ne excitation energy spectrum from one QQQ5 telescope (upper panel) produced by gating on the tritons in Fig. 1. The lower panel shows the locations of previously reported energy levels in ^{19}Ne, taken from Ref. [23].

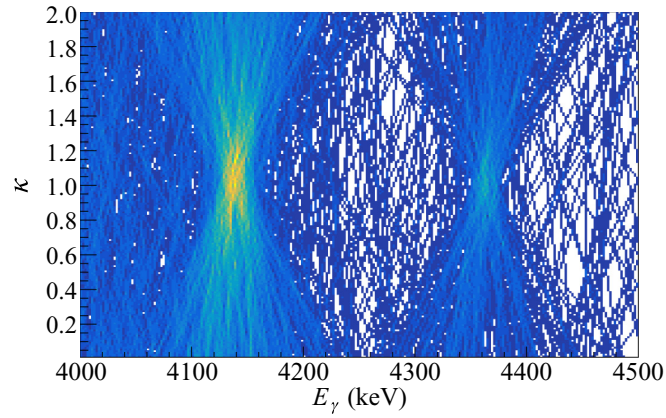

FIG. 3. Gamma-ray spectrum gated on tritons populating excitation energies between 4.0 and 5.0 MeV. The histogram demonstrates how the application of the Doppler correction affects the resolution of the 4140- and 4364-keV γ-ray transitions from the 4377- and 4603-keV ^{19}Ne states, respectively. κ is the fraction of β_{calc} used, and it is clear that short-lived states require the full correction to be applied to minimize the resolution.

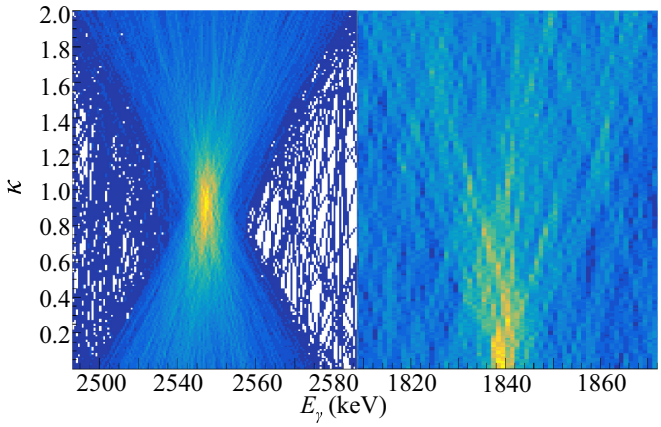

FIG. 4. Gamma-ray spectrum of the 2556-keV transition from the 2794-keV state (left panel) and the 1840-keV transition from the 4634-keV state (right panel). The lifetimes of these states are 100(12) fs and >1 ps, respectively [26]. Therefore, both transitions require a Doppler correction with $\kappa < 1$ to minimize the resolution of the transitions.

the 4377-keV level ($\tau = 5^{+3}_{-2}$ fs [26]) and the 4364-keV transition from the 4603-keV level ($\tau = 7^{+5}_{-4}$ fs [26]). $\beta_{\rm calc}$ ranged from 0.005 to 0.025 depending on the angle of the detected triton. The cumulative Doppler effect from the summation of all of the individual Gammasphere spectra manifests as a general broadening of the peaks using no Doppler correction ($\kappa = 0$). The γ resolution was minimized for short-lived states using $\beta = \beta_{\rm calc}$, demonstrating that ^{19}Ne recoils were typically traveling at full speed when they decayed. The resolution of ^{19}Ne γ-ray transitions was improved by an average factor of 5.0 after applying the correction.

Figure 4 shows transitions from two longer-lived states for comparison. The 2794-keV state, which has a measured lifetime of 100(12) fs, required $\kappa \simeq 0.90$ to minimize the resolution. On the other hand, the 4634-keV state required $\kappa = 0$ due to its long lifetime of >1 ps [26]. In general, $\kappa = 1$ was required to observe the low-statistics transitions from states above 6.0 MeV, as they were assumed to have short lifetimes.

III. RESULTS

A. ^{19}Ne level structure

Figure 5 shows all of the ^{19}Ne levels and γ-ray transitions observed in this work via triton-γ-γ coincidences compared with the level structure of ^{19}F. Mirror states are denoted by dashed lines between the two level schemes. The ^{19}Ne level energies were determined by summing the energies of the γ-ray cascades. In the cases where multiple transitions from the same level were observed, the excitation energies were averaged and weighted by their uncertainties. It should be noted that a recoil correction was not explicitly performed, because the correction was taken into account by the detector calibration. In addition, the recoil energy was generally much smaller than the uncertainties on the measured γ-ray energies. For most transitions, the peak centroids were determined by fitting each peak with a Gaussian and linear background. The γ-ray energy uncertainties were determined by combining the uncertainty from the peak centroid and the uncertainty on the linear calibration of the Gammasphere detectors. The bin widths were also taken into account in the energy uncertainties, especially for low-statistics transitions.

In total, 41 transitions were observed in this work, with 21 of those transitions being newly reported. The bulk of the previously reported γ-ray information came from an analysis of the ^{17}O(^{3}He, $n\gamma$)^{19}Ne reaction by Davidson *et al.* [27], of which only two decays were unobserved in this work (transitions from the 4200 and 4603 keV levels to the 238 and 1536 keV levels, respectively). Notable levels and new transitions are highlighted in the following discussions.

1. Energy levels below 3.0 MeV

In general, all of the energy levels in ^{19}Ne measured below 3.0 MeV match well with previously reported values. Most of the γ-ray cascades from higher-lying states decay through one of the first two excited states at 238 and 275 keV. Therefore, the transitions to the ground state from these low-energy states were used as gates to place coincident γ rays in the ^{19}Ne level scheme. These two transitions, measured with energies of 238.4(3) and 275.4(3) keV, can be seen in Fig. 6(a). Also aiding in the placement of higher-energy γ rays is the fact that the next three states (1508, 1536, and 1616 keV) decay primarily through one of the first two excited states. So, weak γ-ray transitions decaying through one of these three states could be observed and placed by gating on either the 238 or 275-keV γ ray, which have a much higher detection efficiency than γ rays with $E_\gamma > 1.0$ MeV.

The transitions observed for the 1508, 1536, 1616, and 2794-keV states match well with previous measurements. Previously observed transitions to the ground, 238-, and 275-keV states can be found in Fig. 6. One new transition directly to the ground state was observed for the 1536-keV ($J^\pi = 3/2^+$) state with an energy of 1536.8(10) keV (first reported in Ref. [28]) and was subsequently confirmed by Glassman *et al.* [29]. This transition can be found in Fig. 6(d). With this transition, all of the observed transitions in the mirror state [$E_x(^{19}\text{F}) = 1554$ keV] are now reported. In addition, the branching ratios found for these three transitions from the 1536-keV state of 2.2(20)%, 92(2)%, and 5.6(20)% (in order of decreasing γ-ray energy) match well with those reported for the mirror state in ^{19}F of 2.55%, 92.6%, and 4.85% [23].

2. Energy levels between 3.0 and 6.0 MeV

The properties of levels above the α threshold are important inputs to the ^{15}O(α, γ)^{19}Ne reaction in Type I x-ray bursts. The energy of the most important level [$E_x = 4034.4(10)$ keV] was found to be in good agreement with previous measurements. However, the adopted spin-parity assignments for the 4142- and 4200-keV states are inconsistent with the observed γ decays. Their effect on the ^{15}O(α, γ)^{19}Ne reaction was explored in Ref. [24], and more details regarding these spin-parity assignments can be found below. All of the observed transitions from the levels in this excitation energy region can be found in Fig. 7.

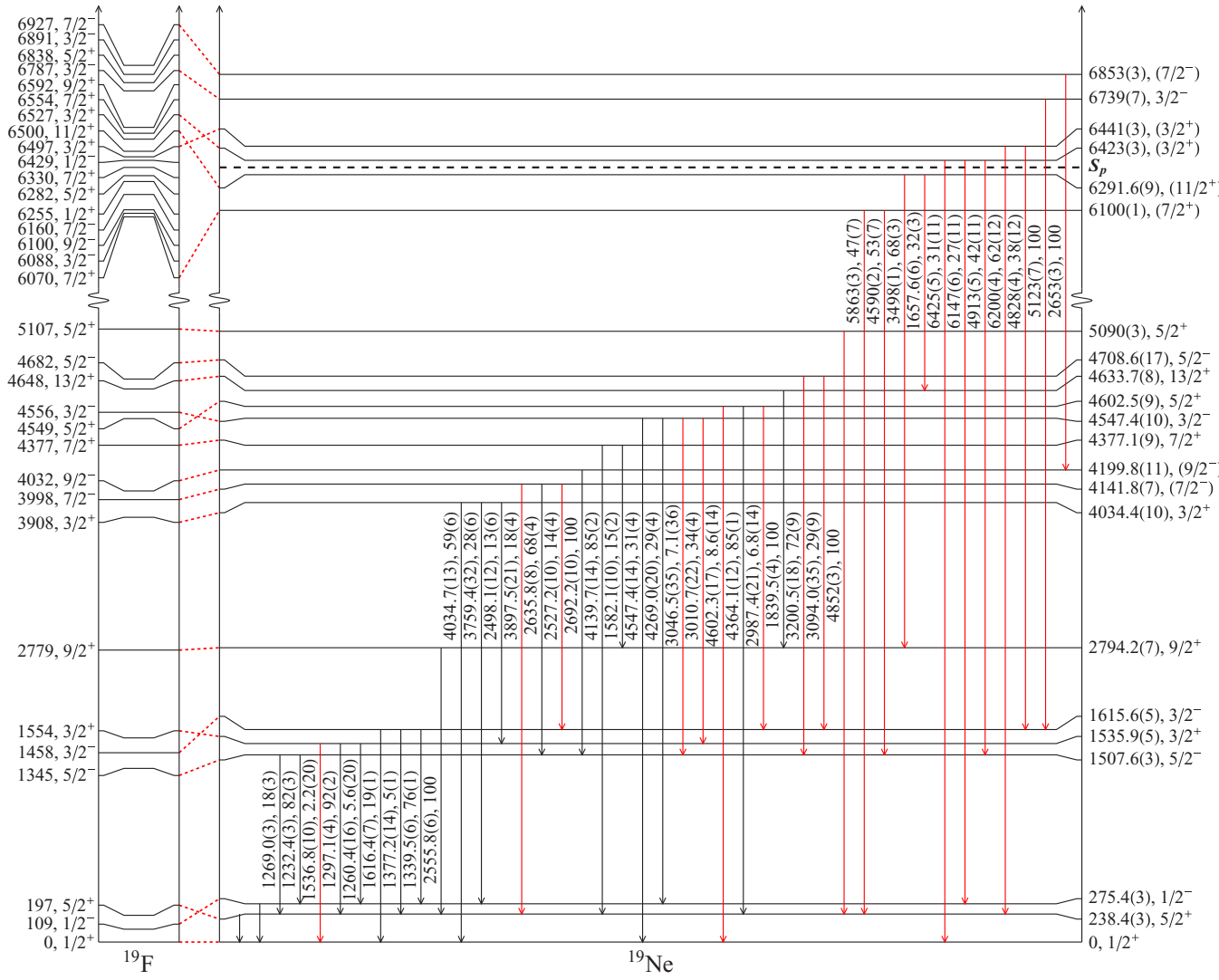

FIG. 5. Level structure of ^{19}Ne for energy levels (keV) observed in the data, with analog states in ^{19}F shown to the left with dashed lines. ^{19}F levels between 5.1 and 6 MeV were omitted for clarity. Transition arrows in black were previously reported. Red arrows signify transitions newly discovered in this work. Gamma-ray energies (keV) and branching ratios (%) are listed next to each transition.

$E_x = 4141.8(7)$ keV, $J^\pi = (7/2^-)$: This level was previously assigned a spin-parity of $9/2^-$ by Davidson *et al.* [27] because expected transitions to the 238- and 1616-keV states were not observed. Parikh *et al.* [12] also agreed with the $9/2^-$ assignment using triton angular distributions measured with the ^{19}F(^{3}He, t)^{19}Ne reaction. However, Tan *et al.* [30] noted that the spin-parity of this state could be $7/2^-$ upon comparisons of the measured lifetime with those reported for states in ^{19}F.

The previously reported 2636-keV transition can be seen in Figs. 7(d) and 7(e). Two γ-ray transitions that were previously unobserved to the 238- and 1616-keV states were measured in this work with energies of 3897.5(21) and 2527.2(10) keV, respectively [see Ref. [24] and Figs. 7(c) and 7(d)]. With these two transitions, the decays from this state closely resemble those found for the 3998 keV state in ^{19}F ($J^\pi = 7/2^-$). The transition to the 1616-keV state ($J^\pi = 3/2^-$) in particular supports the spin-parity assignment made by Ref. [30] of $7/2^-$. The calculated branching ratios of 18(4)%, 68(4)%, and 14(4)% (see Fig. 5) also match well with those observed for the 3998 keV state in ^{19}F of 12%, 70%, and 18% [23].

$E_x = 4199.8(11)$ keV, $J^\pi = (9/2^-)$: Similar to the 4142-keV state, Ref. [27] originally assigned a spin-parity of $7/2^-$ to this state based on an observed transition to the 238-keV state, and Ref. [30] assigned a spin-parity of $9/2^-$ to this state based on measured lifetimes. Since the 4142-keV state was identified as the $7/2^-$ state, we have assigned a spin-parity of $9/2^-$ to this level, making it the mirror of the 4032-keV state in ^{19}F. This assignment is supported by the observed transition to the $5/2^-$1508-keV state, which can be seen in Figs. 7(d) and 7(e). In addition, the $9/2^-$4032-keV state in ^{19}F only decays to the mirror of the $5/2^-$1508-keV state. The previously reported transition to the 238-keV state was not observed in this work.

$E_x = 4547.4(10)$ keV, $J^\pi = 3/2^-$: This state was previously assigned a spin-parity of $3/2^-$ [12], and strong decays observed to the ground state and second-excited state support this assignment [27]. In the current data, two new transi-

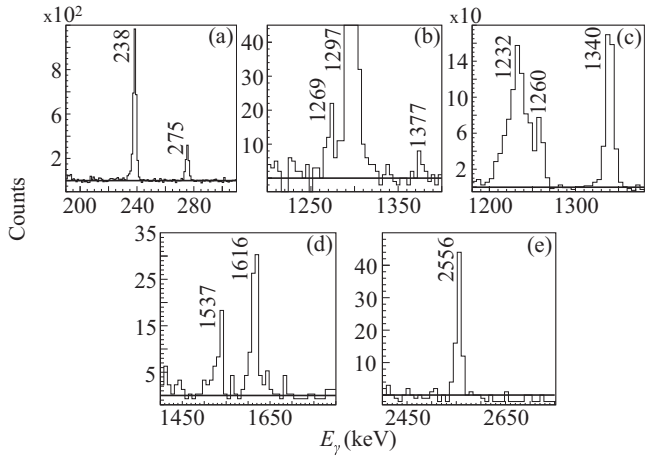

FIG. 6. Random-subtracted low-energy γ-ray spectra showing all transitions observed from states with excitation energies less than 3.0 MeV. All of the spectra were Doppler corrected, except for panel (a), and gated on tritons corresponding to specific ^{19}Ne excitation energy ranges. The E_x ranges and other gating parameters are as follows: (a) 0–0.6 MeV, (b) 1.3–2.1 MeV and the 238-keV γ ray, (c) 1.0–1.8 MeV and the 275-keV γ ray, (d) 1.0–1.8 MeV and a γ-ray multiplicity of 1, (e) 2.0–2.8 MeV and the 238-keV γ ray.

tions were observed depopulating this state in addition to the two previously observed transitions. The new decays to the 1508- and 1536-keV states were measured with energies of 3046.5(35) and 3010.7(22) keV and can be seen in Figs. 7(g) and 7(h), respectively. Based on the assigned mirror level in ^{19}F, two weak decays to the 238- and 1616-keV states should exist but were unobserved. The decay directly to the ground state can be found in Fig. 7(i).

$E_x = 4602.5(9)$ keV, $J^\pi = 5/2^+$: Above 1 GK, this state could provide the most important resonance to the ^{15}O$(\alpha,\gamma)\,^{19}$Ne reaction [30]. The energy measured in this work agrees well with previously measured energies. Two new γ-ray transitions to the ground state [Fig. 7(i)] and 1616-keV state [Fig. 7(j)] were identified in the data with energies of 4602.3(17) and 2987.4(21) keV, respectively.

$E_x = 4708.6(17)$ keV, $J^\pi = 5/2^-$: No transitions had previously been reported from this energy level, but the ^{19}F$(^3$He$, t)\,^{19}$Ne reaction has been shown to populate it [12]. We observe two weak decays to the 1508- and 1616-keV states, which can be seen in Figs. 7(g) and 7(j). The two deexcitations were measured with energies of 3200.5(18) and 3094.0(35) keV and branching ratios of 72(9)% and 29(9)%, respectively. The ^{19}F mirror has been reported as the 4682-keV state, and the relative strengths of these decays in ^{19}Ne match well with those observed for the mirror [23]. This state has the largest difference in energy compared with previous measurements ($E_x = 4712$ keV [12]), but still agrees within the uncertainty.

$E_x = 5090(3)$ keV, $J^\pi = 5/2^+$: The 5107-keV state in ^{19}F had previously been assigned as the mirror of this state based on their similar excitation energies and spin-parity. One new γ-ray transition in coincidence with the 238-keV γ ray was measured with a γ-ray energy of 4852(3) keV [see Fig. 7(k)]. However, this transition has not been observed in the mirror.

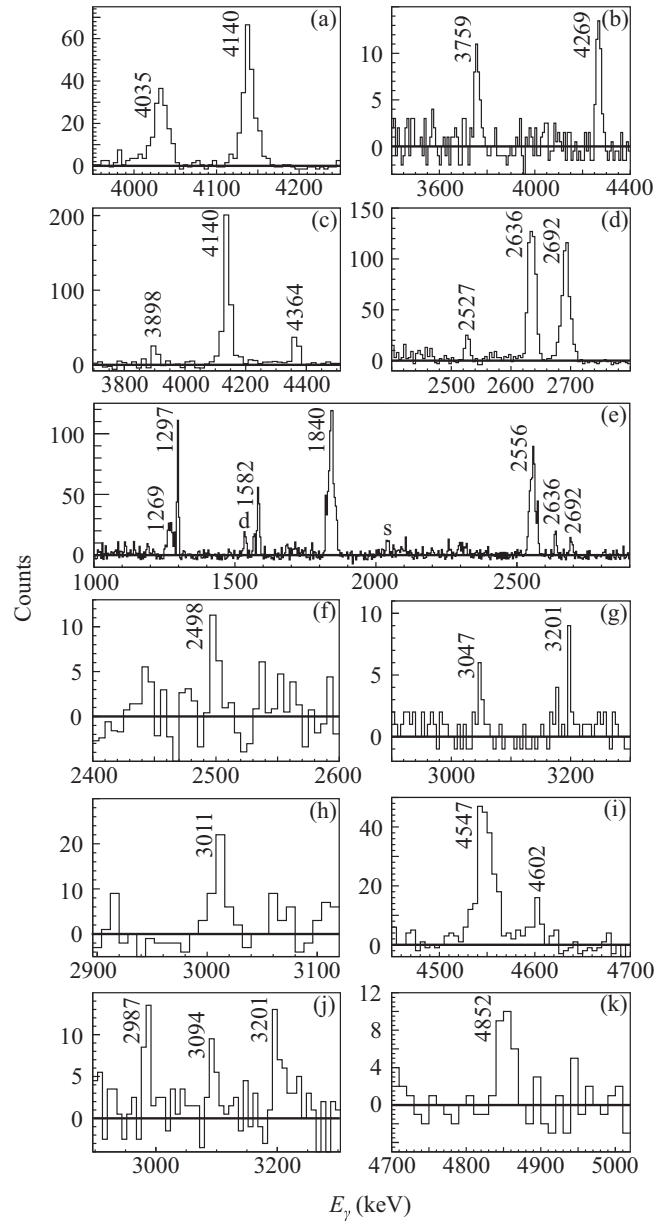

FIG. 7. Random-subtracted γ-ray spectra showing all transitions observed from states between 3.0 and 6.0 MeV. All of the spectra were Doppler corrected and gated on tritons populating specific ^{19}Ne excitation energy ranges. The E_x ranges and other gating parameters are as follows: (a) 3.6–4.4 MeV and a γ-ray multiplicity of 1, (b) 3.8–4.6 MeV and the 275-keV γ ray, (c) 3.7–4.5 MeV and the 238-keV γ ray, (d) 3.7–4.5 MeV and the 275-keV γ ray, (e) 4.0–4.8 MeV and the 238-keV γ ray, (f) 3.8–4.6 MeV and the 1297-keV γ ray, (g) 4.2–5.0 MeV and the 1232-keV γ ray, (h) 4.4–4.9 MeV and the 238-keV γ ray, (i) 4.4–5.2 MeV and a γ-ray multiplicity less than 6, (j) 4.3–5.1 MeV and the 275-keV γ ray, (k) 4.7–5.4 MeV.

3. Energy levels above 6.0 MeV

The ^{19}Ne energy levels above 6.0 MeV are the most interesting for nova nucleosynthesis and have a large influence on the ^{18}F$(p,\alpha)\,^{15}$O reaction rate. The levels near the proton threshold at $S_p = 6410$ keV have been studied extensively by

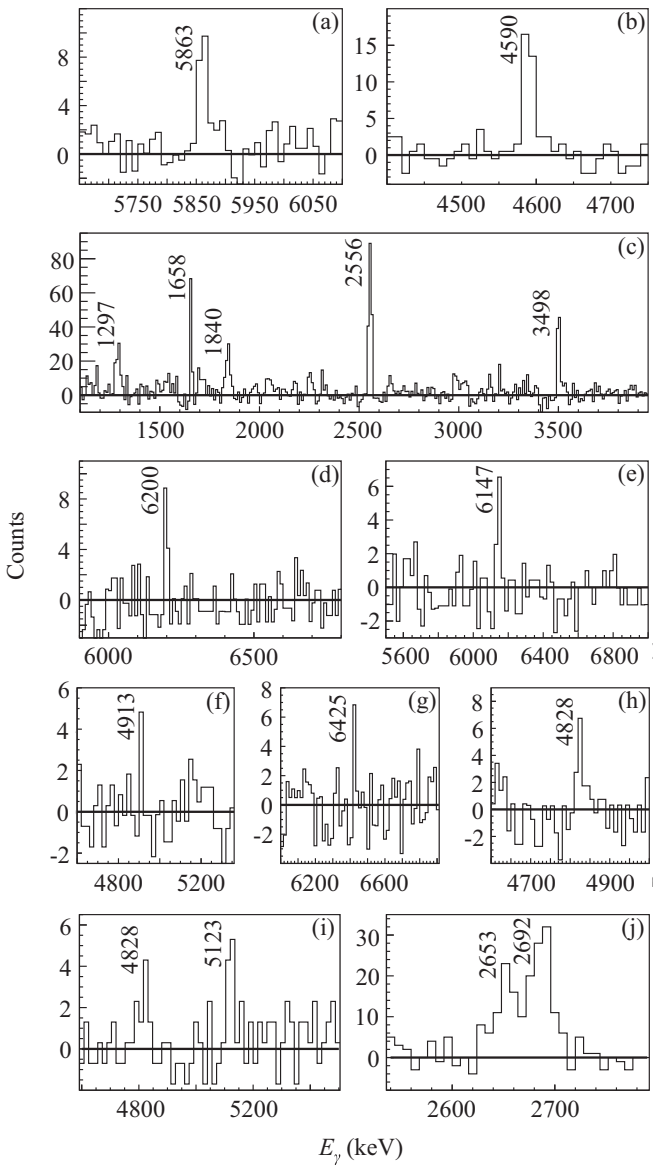

FIG. 8. Random-subtracted γ-ray spectra showing all observed transitions from states above 6.0 MeV. All of the spectra were Doppler corrected and gated on tritons populating specific ^{19}Ne excitation energy ranges. The E_x ranges and other gating parameters are as follows: (a) 5.9–6.7 MeV and the 238-keV γ ray, (b) 5.7–6.5 MeV and the 275-keV γ ray, (c) 5.8–6.6 MeV and the 238-keV γ ray, (d) 6.0–6.8 MeV and the 238-keV γ ray, (e) 6.0–6.5 MeV and the 275-keV γ ray, (f) 6.0–6.5 MeV and the 1232-keV γ ray, (g) 6.2–7.0 MeV and a γ-ray multiplicity of 1, (h) 5.7–6.5 MeV and the 275-keV γ ray, (i) 6.4–7.0 MeV and the 275-keV γ ray, (j) 6.5–7.0 MeV and the 1232-keV γ ray.

a variety of charged-particle experiments [3,7,12], yet still remain one of the most important sources of uncertainty in the rate. No γ-ray decay information had been reported for these levels previously. We observe a total of nine deexcitations from six levels in the region above 6.0 MeV and the results are summarized below. In addition, all of the observed transitions can be found in Fig. 8.

$E_x = 6100(1)$ keV, $J^\pi = (7/2^+)$: A state with a similar excitation energy was observed using the ^{19}F(^{3}He, t)^{19}Ne reaction by Refs. [3,7]. A spin-parity of $7/2^+$ or $9/2^+$ was assigned to this state by Ref. [7]; however, it is likely to be $7/2^+$ based on the structure of ^{19}F in this energy region [$E_x(^{19}\text{F}) = 6070$ keV]. In addition, there are no known $9/2^+$ states in ^{19}F between $E_x = 2.8$ and 6.5 MeV. We observe two deexcitations from this state in the data to the 238- and 1508-keV states with energies of 5863(3) keV [see Fig. 8(a)] and 4590(2) keV [see Fig. 8(b)]. Two of the three strongest transitions observed for the 6070-keV state in ^{19}F are to the mirrors of the 238- and 1508-keV ^{19}Ne states, which further supports this mirror assignment.

$E_x = 6291.6(9)$ keV, $J^\pi = (11/2^+)$: A well-known subthreshold resonance ($J^\pi = 1/2^+$) has been found close to this excitation energy at $E_x = 6286(3)$ keV [5,8]. However, Ref. [7] observed a state in this region at 6289 keV that could not be reproduced using a low spin-parity. Subsequent analysis by Parikh *et al.* [12] explored the idea that the state found by Ref. [7] could be a doublet with energies of 6282 and 6295 keV, although they did not propose any spin-parity assignments.

No evidence for the $1/2^+$ state was observed in the γ-ray spectra, but γ rays from a high-spin state with an excitation energy of $E_x = 6291.6(9)$ keV were detected. Transitions with energies of 3498(1) and 1657.6(6) keV were found in coincidence with γ rays from the energy levels at 2794 ($J^\pi = 9/2^+$) and 4634 keV ($J^\pi = 13/2^+$), respectively [see Fig. 8(c)]. Comparing these two decays with known decays in ^{19}F suggests a mirror connection between this state and the 6500-keV state in ^{19}F, which has a spin-parity of $11/2^+$. The decay to the $13/2^+$ state at 4634 keV is especially important in the spin-parity determination, because all of the states in ^{19}F reported to decay to the $13/2^+$ mirror state at 4648 keV have $J \geqslant 11/2$.

$E_x = 6423(3)$ keV, $J^\pi = (3/2^+)$: The first above-threshold state observed in the data is at 6423(3) keV, which corresponds to a resonance energy of $E_r = 13(3)$ keV. States with energies of 6419(6) keV [3,5] and 6416(3) keV [7] were observed in previous measurements, and spins of $3/2^-$ or $5/2^+$ were determined for these states using angular distribution data [5,7]. However, a ^{19}F mirror was not suggested, and no $3/2^-$ or $5/2^+$ states have been observed with excitation energies between 6.3 and 6.7 MeV in ^{19}F.

Three transitions were observed in the data from this level. A deexcitation with an energy of 6425(5) keV was observed [see Fig. 8(g)] and was not in coincidence with γ rays from lower-energy states. Therefore, we have identified this transition as the transition from the 6423-keV state to the ground state. The second transition from this level has an energy of 6147(6) keV and was observed to be in coincidence with decays from the 275-keV state [see Fig. 8(e)]. The third transition was found with an energy of 4913(5) keV in coincidence with the 1233-keV γ-ray line from the 1507-keV state [see Fig. 8(f)]. The relative branching ratios for these three decays were determined to be 31(11)%, 27(11)%, and 42(11)%, respectively.

Since the spin-parity of the 275-keV state is $1/2^-$, a low spin-parity for the 6423-keV state is implied and is constrained to be $J \leqslant 5/2$. The two $3/2^+$ states in ^{19}F at 6497 and 6527 keV have a similar decay pattern to the transitions observed for this state, and the absence of an obvious $3/2^-$ or $5/2^+$ mirror level in ^{19}F suggests a spin-parity of $3/2^+$.

$E_x = 6441(3)$ keV, $J^\pi = (3/2^+)$: This state would correspond to a resonance at $E_r = 31(3)$ keV. Excited states with excitation energies of 6450(6) keV [3] and 6440(3) keV [7] have been previously reported near this excitation energy. Laird *et al.* [7] assigned a spin-parity of $11/2^+$ to the 6440-keV state observed in their work. The γ-ray transitions observed in this work for this state and the 6291-keV state suggest that the spin-parity of the 6440-keV state is not $11/2^+$, since the only the $11/2^+$ state in ^{19}F below 7.0 MeV has now been accounted for in ^{19}Ne.

Two transitions to the 238- and 1616-keV states were observed with energies of 6200(4) and 4828(4) keV and branching ratios of 62(12)% and 32(12)%, respectively. The 6200-keV transition can be seen in Fig. 8(d) and was found to be in coincidence with transitions from the 238 keV state. The 4828-keV transition was found in coincidence with the 275-keV transition [see Figs. 8(h) and 8(i)], which the 1616 keV state primarily decays through. Since the spin-parities of the 238- and 1616-keV states are $5/2^+$ and $3/2^-$, respectively, the 6441-keV state most likely has a spin $J \leqslant 7/2$. Looking at the available states and observed γ decays in the mirror, a $3/2^+$ spin-parity is suggested.

The $E_x = 6496$-keV $3/2^+$ state in ^{19}F has been observed to decay to the mirrors of the 238-, 275-, 1508-, and 1616-keV states, whereas a decay to the mirror of the 1616-keV state has not been observed from the 6527-keV $3/2^+$ state in ^{19}F [23]. Therefore, we assign the 6441-keV ^{19}Ne state as the mirror of the 6496-keV ^{19}F state. It should be noted, however, that these mirror assignments do not affect the following conclusions found for the ^{18}F$(p,\alpha)^{15}$O reaction rate in this analysis since the widths used were not calculated using the ^{19}F level properties.

$E_x = 6739(7)$ keV, $J^\pi = 3/2^-$: This state has been shown previously to be important in the ^{18}F$(p,\alpha)^{15}$O reaction-rate calculation ($\ell = 1$) [31]. The properties of this state have been constrained in previous measurements by Bardayan *et al.* [32] and more recently by Beer *et al.* [6]. One transition was observed in the present analysis with an energy of 5123(7) to the 1616-keV state, when gated on the 275-keV γ ray, and can be seen in Fig. 8(i). Due to the limited statistics for this transition, the level-energy uncertainty is higher than previous measurements for this state, so the reaction-rate calculations performed in the next section use the better-constrained value of the resonance energy from Ref. [8] of $E_r = 332(2)$ keV.

$E_x = 6853(3)$ keV, $J^\pi = (7/2^-)$: An energy level in a similar location has been previously observed by ^{19}F$(^3$He$, t)^{19}$Ne reaction experiments [7,12], and Ref. [12] explored the possibility of a doublet in their data having constituent energies of 6851 and 6864 keV. One transition was observed in the current experiment at 2653(3) keV when gating on tritons between $E_x = 6.4$ and 7.0 MeV and the 1233-keV γ-ray transition from the 1508-keV state [see Fig. 8(j)]. This transition was placed in the level scheme as a decay to the 4200-keV state, which gives an initial level energy of 6853 keV. The other likely option is a decay to the 4142-keV state, but in this case the initial level energy does not line up with any of the states observed by previous measurements. In addition, the decay from the 4142-keV state to the 1508-keV state only has a measured branching ratio of 18(4)%, making the observation of the 2653-keV γ ray in coincidence with the 1233-keV transition less likely.

B. ^{18}F$(p,\alpha)^{15}$O reaction-rate calculations

The observed properties of the levels near the proton threshold discussed in the previous section were used to better constrain the ^{18}F$(p,\alpha)^{15}$O reaction rate. In addition to the level energies, the proton and α widths (Γ_p and Γ_α) are necessary to calculate the rate. Since they were not measured in this experiment, the widths from previous measurements were scaled to the new excitation energies. The width can be estimated using the following equation [33,34]:

$$\Gamma_\ell(E) = \frac{2\hbar c}{R_n}\left[\frac{2E}{\mu c^2}\right]^{1/2} P_\ell(E, R_n)\theta_\ell^2, \tag{2}$$

where Γ_ℓ is the partial width, ℓ is the angular momentum, R_n is the radius, E is the excitation energy, μ is the reduced mass of the ^{18}F $+p$ system, θ_ℓ^2 is the reduced width, and P_ℓ is the penetration factor. The partial widths were calculated for the previously observed and newly measured energies, and the ratio of the calculated widths was used to scale the previously measured partial widths.

Although not necessary for the rate calculations, γ partial widths were also calculated for the levels observed from previous measurements of Γ_γ for mirror states in ^{19}F. This was done via [34]

$$(\Gamma_\gamma)_{^{19}\mathrm{Ne}} = \left[\frac{E_\gamma(^{19}\mathrm{Ne})}{E_\gamma(^{19}\mathrm{F})}\right]^{(2L+1)}\left[\frac{B(L)(^{19}\mathrm{Ne})}{B(L)(^{19}\mathrm{F})}\right](\Gamma_\gamma)_{^{19}\mathrm{F}}, \tag{3}$$

where E_γ is the transition energy, L is the multipolarity of the transition, and $B(L)$ is the reduced transition probability. In most cases, more transitions from the suspected mirror level in ^{19}F were reported, so to scale the partial widths for these levels in ^{19}Ne, E_γ was calculated using the measured energies of the initial and final levels.

A summary of the energy levels and partial widths necessary for the reaction-rate calculation can be found in Table I. Well-established states from previous measurements were considered alongside the states found in this work. The $\ell = 0$ resonance observed by Kahl *et al.* [17] was not included in the calculations, because no γ-ray transitions were observed from this state, and no significant strength to populate this state was observed in the ^{18}F$(d,n)^{19}$Ne measurements [5]. However, the resonance could be significant depending on its properties, as thoroughly investigated by Ref. [17] and noted below.

The proton partial widths and spectroscopic factors for the two above-threshold $3/2^+$ states were constrained using the ^{18}F$(d,n)^{19}$Ne experiment by Adekola *et al.* [5]. The $3/2^+$ states were not found in the Ref. [5] measurement, but upper limits for the partial width and spectroscopic factor, assum-

TABLE I. ^{19}Ne resonance parameters used for the ^{18}F$(p,\alpha)^{15}$O reaction-rate calculation.

^{19}Ne							^{19}F[a]			
E_x (keV)	E_r (ke)	J^π	Γ_γ (eV)	θ_p^2	Γ_p (keV)	Γ_α (keV)	E_x (keV)	Γ_γ (eV)	Γ_α (keV)	$\Gamma_{\rm tot}$ (keV)
6286(3)[b]	−124	$\frac{1}{2}^+$			83.5[c]	11.6				
6416(4)[d]	6	$\frac{3}{2}^-$			2.8×10^{-27}	<0.5				
6423(3)[e]	13	$\frac{3}{2}^+$	1.1(6)	⩽0.028	$\leqslant 3.9\times10^{-29}$	1.2	6528	1.2	1.2	1.2
6439(3)[d]	29	$\frac{1}{2}^-$		0.01	$\leqslant 3.8\times10^{-19}$	220	6536		245	245
6441(3)[e]	31	$\frac{3}{2}^+$	0.79(40)	⩽0.028	$\leqslant 8.4\times10^{-18}$	1.3	6497	0.85	0.5	0.5
6459(5)[d]	49	$\frac{5}{2}^-$			8.4×10^{-14}	5.5				
6699(3)[d]	289	$\frac{5}{2}^+$	0.29(15)	0.01	2.4×10^{-5}	1.2	6838	0.33	1.2	1.2
6742(2)[d]	332	$\frac{3}{2}^-$	5.0(26)		2.22×10^{-3}	5.2	6787	5.5	4.3	4.3
7075(2)[d]	665	$\frac{3}{2}^+$			15.2	23.8	(7300)			
7871(19)[d]	1461	$\frac{1}{2}^+$			55	347				

[a]All ^{19}F parameters taken from Nesaraja *et al.* [34]. Γ_γ for ^{19}Ne scaled from those shown for ^{19}F.
[b]Γ_p and Γ_α scaled from those reported in Bardayan *et al.* [8].
[c]ANC (fm$^{1/2}$).
[d]Γ_p and Γ_α scaled from those reported in Laird *et al.* [7].
[e]Γ_p scaled from upper limit reported in A. S. Adekola *et al.* [5].

ing an excitation energy of 6449 keV, were determined to be $\Gamma_p \leqslant 2.35\times10^{-15}$ keV and $S_p \leqslant 0.028$. In the following reaction-rate calculations, it was assumed that the majority of the spectroscopic strength was in one of the two $3/2^+$ states. Because the α partial widths are much larger than the proton partial widths, they are less important and have a negligible effect on the reaction-rate calculation. Nevertheless, the α partial widths presented in Table I were scaled from those presented in Ref. [8].

The *R*-matrix code AZURE2 [35] was used to investigate the uncertainties in the *S* factor due to interference between the broad $1/2^+$ ($E_x = 7871$ keV) and $3/2^+$ states ($E_x = 7075$ keV) and the lower-lying states with the same spin-parity. Interference was not considered between the two $3/2^-$ states (see Table I) because the two levels do not overlap.

Figure 9 shows the result of the calculation using various combinations for the signs of the partial widths. The first set of parentheses shows the signs on the partial widths for the two $1/2^+$ states, and the second shows the signs on the partial widths for the three $3/2^+$ states. Included in the calculation was a 15-keV experimental energy resolution to compare with previously published *S*-factor measurements [6,11,32,36].

Previous predictions of the ^{18}F$(p,\alpha)^{15}$O reaction rate were widely varying due to conflicting results for the energies of the near-threshold $3/2^+$ states. However, the locations of the mirror states above the proton threshold were predicted by Nesaraja *et al.* [34] to be lower in energy than those in ^{19}F by 50 ± 30 keV. Therefore, prior to the current analysis, the best estimates for the energies of the $3/2^+$ states were 6447 ± 30 and 6477 ± 30 keV from the 6497- and 6527-keV ^{19}F states, respectively.

To calculate the reaction-rate uncertainties, the energy of each level was allowed to vary within their energy uncertainties, while scaling Γ_p and Γ_α accordingly. The interference signs for the maximum and minimum rate bands were $(-+)(--+)$ and $(++)(+++)$, respectively. Figure 10 shows the rate bands calculated using the previous best estimate for the two $3/2^+$ states (red dashed lines) and the rate calculated using the constrained energies found in this work (black solid line). The blue dashed-dotted lines show the reaction rate calculated by Bardayan *et al.* [8] for comparison, which only considered one $3/2^+$ state near the proton threshold at 6457 keV.

The upper limit of the rate was greatly constrained by determining the energies of the near-threshold $3/2^+$ states. The red hatched area in Fig. 10 represents the values of the rate that can be excluded by constraining the $3/2^+$ states. At nova temperatures (0.1 to 0.25 GK), the upper limit of the

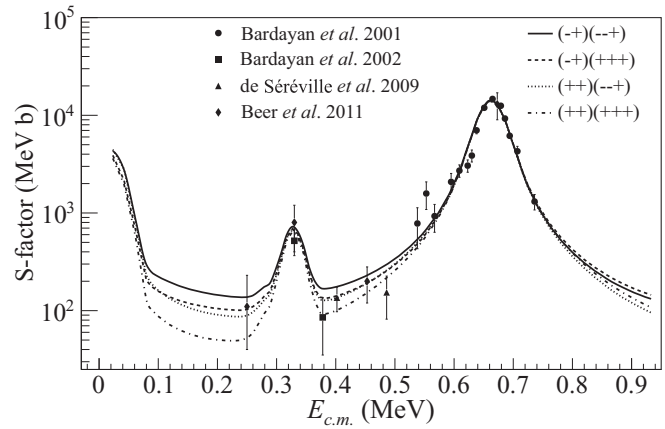

FIG. 9. *S* factors calculated for the ^{18}F$(p,\alpha)^{15}$O reaction assuming the combination of interference signs shown. The first (second) set of parentheses shows the interference signs for the $1/2^+$ ($3/2^+$) states. An energy resolution of 15-keV was included for comparison with experimental data from Bardayan 2001 [11], Bardayan 2002 [32], de Séréville 2009 [36], and Beer 2011 [6]. This figure was adapted from Ref. [9].

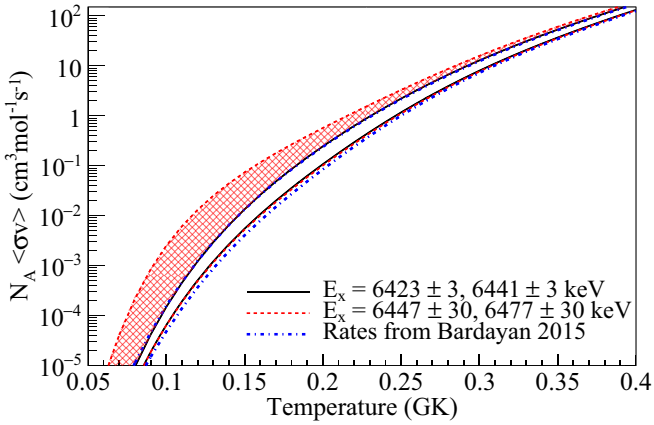

FIG. 10. ^{18}F$(p,\alpha)^{19}$Ne reaction rate calculations showing the reduction in uncertainty from constraining the energies of the $3/2^+$ states. The upper limit of the rate is reduced by factors of 1.5–17 in the temperature range of nova nucleosynthesis. The rate calculated by Bardayan 2015 [8] is included for comparison. This figure was adapted from Ref. [9].

rate was reduced by factors of 1.5 to 17, meaning a higher annihilation radiation flux due to the increased amount of ^{18}F left in the envelope of the explosion. Inclusion of a fourth $3/2^+$ state at 6130 keV ($E_r = -280$ keV) using the ANC and α width hypothesized by Kahl *et al.* [17] raises (lowers) the upper (lower) limit by <7.5% in the nova temperature range.

The new rate bands presented are very close to those calculated previously by Bardayan *et al.* [8]. Figure 11 shows the ratio of each limit to the upper limit from Ref. [8]. Assuming most of the spectroscopic strength measured by Ref. [5] was in the $E_r = 31$-keV resonance gave the largest rate uncertainties, which means the inclusion of the $E_r = 13$-keV resonance ultimately had a very small effect on the reaction rate. This is demonstrated by the similarity between the limits from this analysis and the limits from Ref. [8], where only a single $3/2^+$ state at $E_r = 47$ keV was considered. However, the $E_r = 47$ keV resonance used by Ref. [8] was speculated based on previous measurements, so determining the resonance energies

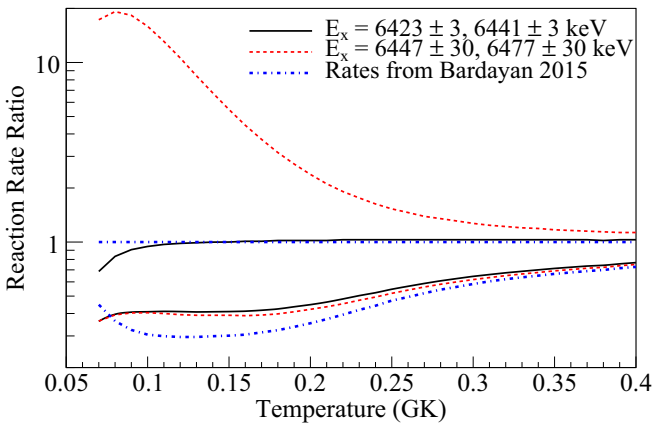

FIG. 11. Ratios of the ^{18}F$(p,\alpha)^{19}$Ne reaction rates from Fig. 10 to the upper limit from Bardayan 2015 [8].

precisely considerably reduces the uncertainty in the reaction rate, assuming consistent properties for the levels.

C. Nova nucleosynthesis calculations

With the upper and lower limits of the ^{18}F$(p,\alpha)^{19}$Ne reaction rate better constrained, nucleosynthesis calculations were performed to assess how the reduction in reaction-rate uncertainties affects the amount of ^{18}F left in the envelope of the explosion to decay. The Computational Infrastructure for Nuclear Astrophysics (CINA) [37] was used, which simulates the evolution of nova abundances through time profiles of temperature and density taken from one-dimensional (1D) hydrodynamic model calculations [38], broken into radial zones. Isotopic abundances between ^{1}H and ^{54}Cr are tracked during the simulation.

To use the calculated upper and lower limits of the rate, they were parametrized using the following equation [39]:

$$N_A\langle\sigma v\rangle = \sum_{j=0}^{1} \exp\left[a_{0j} + \sum_{i=1}^{5} a_{ij} T_9^{(2i-5)/3} + a_{6j} \ln T_9\right], \quad (4)$$

where $a_{i,j}$ are the coefficients used to fit the rate and T_9 is the temperature in GK. The coefficients for the newly constrained upper and lower limits of the rate are presented in Table II. The parametrization is valid between temperatures of 0.1 and 0.4 GK to within 5% and was extended to be valid from 0.01 to 10 GK. However, it should be noted that higher-energy resonance information was not included in the reaction-rate calculation. The parametrized rates were then combined with reaction rates from the REACLIB v2.0 library [39]. Nucleosynthesis calculations using the old and new upper and lower limits of the ^{18}F$(p,\alpha)^{19}$Ne rate were performed on a CO white dwarf with a mass of 1.0 solar masses, and on ONeMg white dwarfs with masses of 1.15, 1.25, and 1.35 solar masses.

From the simulations, the uncertainty in the ^{18}F abundance was reduced by factors of 2.5, 2.6, 2.5, and 2.4 in order of increasing white dwarf mass. Since the upper limit of the rate was reduced at all temperatures, the simulations using the newly constrained rates generally predict more ^{18}F left over in the envelope to decay and hence a higher γ-ray flux. Therefore, the distance that a nova explosion can be detected using the annihilation radiation must also be increased.

The detectors on a γ-ray observatory have a minimum γ-ray flux required to detect an astrophysical event. Using this minimum flux requirement, the uncertainties in the maximum detectability range and detection probability can also be estimated. Assuming that the simulated ^{18}F abundance corresponds directly to the annihilation radiation flux, the uncertainty on the maximum detectable range is reduced by a factor of 3.3 on average. Similarly, the uncertainty in the probability of event detection is reduced by a factor of 2.1 on average.

IV. CONCLUSIONS

The energy levels of ^{19}Ne are important in the reaction-rate calculations of the ^{15}O$(\alpha,\gamma)^{19}$Ne reaction in Type I x-ray bursts and the ^{18}F$(p,\alpha)^{15}$O reaction in novae. The unknown

TABLE II. Reaction-rate parametrization coefficients a_{ij}, valid between temperatures of 0.1–0.4 GK.

	High		Low	
j/i	0	1	0	1
0	0.281708×10^4	0.760966×10^2	0.796387×10^2	0.304808×10^4
1	-0.253893×10^1	0.200131×10^1	0.207772×10^1	-0.236511×10^1
2	0.533284×10^3	-0.130412×10^3	-0.133803×10^3	0.536582×10^3
3	-0.430696×10^4	0.665259×10^2	0.660557×10^2	-0.466364×10^4
4	0.149924×10^4	-0.121037×10^1	-0.997821×10^0	0.171984×10^4
5	-0.577818×10^3	0.654131×10^{-2}	-0.854160×10^{-2}	-0.688736×10^3
6	0.906714×10^3	-0.565037×10^2	-0.575115×10^2	0.947794×10^3

location of two $3/2^+$ states near 6.4 MeV, which exist in the mirror nucleus ^{19}F, were a major source of uncertainty in the ^{18}F$(p,\alpha)^{15}$O reaction rate, which is responsible for destruction of ^{18}F. Gammasphere ORRUBA: Dual Detectors for Experimental Structure Studies was used to study the energy levels in ^{19}Ne with the ^{19}F$(^3$He$, t)^{19}$Ne reaction. In total, 41 transitions from 21 energy levels were measured, including 21 new transitions. Two levels just above the proton threshold in ^{19}Ne ($E_x = 6423$ and 6441 keV) were identified as likely candidates for the $3/2^+$ states of interest. In addition, the γ rays observed for the 4142- and 4200-keV states, which are resonances in the ^{15}O$(\alpha,\gamma)^{19}$Ne reaction, resolve a discrepancy in their previous spin-parity assignments.

S-factor and reaction-rate calculations were performed to determine how the newly constrained levels affect the ^{18}F$(p,\alpha)^{15}$O reaction rate. It was found that the upper limit of the rate is reduced by factors of 1.5–17 at nova temperatures, which increases estimates for the amount of ^{18}F left over to β^+ decay after the explosion. Nova nucleosynthesis calculations were performed on white dwarfs of various masses, and the uncertainty in the ^{18}F abundance was reduced by an average factor of 2.5. This also reduces the uncertainty on the maximum detectable range of a nova explosion by a factor of 3.3 on average. Additional studies in the future should focus on further confirming the location and spin-parities of the above-threshold states, as well as measurements of the *S* factor to determine the signs of the interference between the levels.

ACKNOWLEDGMENTS

This research was supported in part by the National Science Foundation Grants No. PHY-1419765 (Notre Dame) and No. PHY-1404218 (Rutgers), the National Nuclear Security Administration under the Stewardship Science Academic Alliances program through Department of Energy Cooperative Agreement DE-NA002132, and by the National Research Foundation of Korea (NRF) grant funded by the Korea government (MSIT) (No. NRF-2016R1A5A1013277, No. NRF-2020R1A2C1005981, and No. NRF-2013M7A1A1075764). The authors also acknowledge support from the DOE Office of Science, Office of Nuclear Physics, under Contracts No. DE-AC05-00OR22725, No. DE-FG02-96ER40963, No. DE-FG02-96ER40978, No. DE-AC02-06CH11357, and No. DE-AC02-98CH10886. This research used resources of Argonne National Laboratory's ATLAS facility, which is a DOE Office of Science User Facility.

[1] R. Wallace and S. Woosley, Astrophys. J., Suppl. Ser. **45**, 389 (1981).
[2] H. Schatz, A. Aprahamian, J. Görres, M. Wiescher, T. Rauscher, J. Rembges, F.-K. Thielemann, B. Pfeiffer, P. Möller, K.-L. Kratz *et al.*, Phys. Rep. **294**, 167 (1998).
[3] S. Utku, J. G. Ross, N. P. T. Bateman, D. W. Bardayan, A. A. Chen, J. Görres, A. J. Howard, C. Iliadis, P. D. Parker, M. S. Smith *et al.*, Phys. Rev. C **57**, 2731 (1998).
[4] J. José and S. Shore, in *Classical Novae*, edited by M. F. Bode and A. Evans (Cambridge University Press, Cambridge, 2008).
[5] A. S. Adekola, D. W. Bardayan, J. C. Blackmon, C. R. Brune, K. Y. Chae, C. Domizioli, U. Greife, Z. Heinen, M. J. Hornish, K. L. Jones *et al.*, Phys. Rev. C **83**, 052801(R) (2011).
[6] C. E. Beer, A. M. Laird, A. St. J. Murphy, M. A. Bentley, L. Buchmann, B. Davids, T. Davinson, C. A. Diget, S. P. Fox, B. R. Fulton *et al.*, Phys. Rev. C **83**, 042801(R) (2011).
[7] A. M. Laird, A. Parikh, A. St. J. Murphy, K. Wimmer, A. A. Chen, C. M. Deibel, T. Faestermann, S. P. Fox, B. R. Fulton, R. Hertenberger *et al.*, Phys. Rev. Lett. **110**, 032502 (2013).
[8] D. W. Bardayan, K. A. Chipps, S. Ahn, J. C. Blackmon, R. J. deBoer, U. Greife, K. L. Jones, A. Kontos, R. L. Kozub, L. Linhardt *et al.*, Phys. Lett. B **751**, 311 (2015).
[9] M. R. Hall, D. W. Bardayan, T. Baugher, A. Lepailleur, S. D. Pain, A. Ratkiewicz, S. Ahn, J. M. Allen, J. T. Anderson, A. D. Ayangeakaa *et al.*, Phys. Rev. Lett. **122**, 052701 (2019).
[10] D. W. Bardayan, J. C. Blackmon, J. Goez del Campo, R. L. Kozub, J. F. Liang, Z. Ma, L. Sahin, D. Shapira, and M. S. Smith, Phys. Rev. C **70**, 015804 (2004).
[11] D. W. Bardayan *et al.*, Phys. Rev. C **63**, 065802 (2001).
[12] A. Parikh, A. M. Laird, N. de Séréville, K. Wimmer, T. Faestermann, R. Hertenberger, D. Seiler, H. -F. Wirth, P. Adsley, B. R. Fulton *et al.*, Phys. Rev. C **92**, 055806 (2015).
[13] N. de Séréville, E. Berthoumieux, and A. Coc, Nucl. Phys. A **758**, 745c (2005).
[14] R. L. Kozub, D. W. Bardayan, J. C. Batchelder, J. C. Blackmon, C. R. Brune, A. E. Champagne, J. A. Cizewski, T. Davinson, U. Greife *et al.*, Phys. Rev. C **71**, 032801(R) (2005).

[15] A. S. Adekola, C. R. Brune, D. W. Bardayan, J. C. Blackmon, K. Y. Chae, C. Domizioli, U. Greife, Z. Heinen, M. J. Hornish, K. L. Jones *et al.*, Phys. Rev. C **84**, 054611 (2011).
[16] A. S. Adekola, C. R. Brune, D. W. Bardayan, J. C. Blackmon, K. Y. Chae, J. A. Cizewski, K. L. Jones, R. L. Kozub, T. N. Massey, C. D. Nesaraja *et al.*, Phys. Rev. C **85**, 037601 (2012).
[17] D. Kahl, P. J. Woods, Y. Fujita, H. Fujita, K. Abe, T. Adachi, D. Frekers, T. Ito, N. Kikukawa, M. Nagashima *et al.*, Eur. Phys. J. A **55**, 4 (2019).
[18] A. Ratkiewicz, S. D. Pain, J. A. Cizewski, D. W. Bardayan, J. C. Blackmon, K. A. Chipps, S. Hardy, K. L. Jones, R. L. Kozub, C. J. Lister *et al.*, AIP Conf. Proc. **1525**, 487 (2013).
[19] S. D. Pain, A. Ratkiewicz, T. Baugher, M. Febbraro, A. Lepailleur, A. D. Ayangeakaa, J. Allen, J. T. Anderson, D. W. Bardayan, J. C. Blackmon *et al.*, Phys. Procedia **90**, 455 (2017).
[20] S. D. Pain, J. A. Cizewski, R. Hatarik, K. L. Jones, J. S. Thomas, D. W. Bardayan, J. C. Blackmon, C. D. Nesaraja, M. S. Smith, R. L. Kozub *et al.*, Nucl. Instrum. Methods Phys. Res., Sect. B **261**, 1122 (2007).
[21] I.-Y. Lee, Nucl. Phys. A **520**, c641 (1990).
[22] M. R. Hall, D. W. Bardayan, T. Ahn, J. M. Allen, J. T. Anderson, A. D. Ayangeakaa, T. Baugher, J. C. Blackmon, D. Blankstein, S. Burcher *et al.*, AIP Conf. Proc. **2160**, 070009 (2019).
[23] D. R. Tilley, H. R. Weller, C. M. Cheves, and R. M. Chasteler, Nucl. Phys. A **595**, 1 (1995).
[24] M. R. Hall, D. W. Bardayan, T. Baugher, A. Lepailleur, S. D. Pain, A. Ratkiewicz, S. Ahn, J. M. Allen, J. T. Anderson, A. D. Ayangeakaa *et al.*, Phys. Rev. C **99**, 035805 (2019).
[25] M. R. Hall, D. W. Bardayan, T. Baugher, A. Lepailleur, S. D. Pain, A. Ratkiewicz, S. Ahn, J. M. Allen, J. T. Anderson, A. D. Ayangeakaa *et al.*, Phys. Rev. C **101**, 015804 (2020).
[26] W. P. Tan, J. Görres, J. Daly, M. Couder, A. Couture, H. Y. Lee, E. Stech, E. Strandberg, C. Ugalde, and M. Wiescher, Phys. Rev. C **72**, 041302(R) (2005).
[27] J. M. Davidson and M. L. Roush, Nucl. Phys. A **213**, 332 (1973).
[28] M. R. Hall, Ph.D. thesis, University of Notre Dame, 2018 (unpublished).
[29] B. E. Glassman, D. Peŕez-Loureiro, C. Wrede, J. Allen, D. W. Bardayan, M. B. Bennett, K. A. Chipps, M. Febbraro, M. Friedman, C. Fry *et al.*, Phys. Rev. C **99**, 065801 (2019).
[30] W. P. Tan, J. Görres, M. Beard, M. Couder, A. Couture, S. Falahat, J. L. Fisker, L. Lamm, P. J. LeBlanc, H. Y. Lee *et al.*, Phys. Rev. C **79**, 055805 (2009).
[31] M. Wiescher and K.-U. Kettner, Astrophys. J. **263**, 891 (1982).
[32] D. W. Bardayan *et al.*, Phys. Rev. Lett. **89**, 262501 (2002).
[33] C. E. Rolfs and W. S. Rodney, *Cauldrons in the Cosmos* (The University of Chicago Press, Chicago, 1988).
[34] C. D. Nesaraja, N. Shu, D. W. Bardayan, J. C. Blackmon, Y. S. Chen, R. L. Kozub, and M. S. Smith, Phys. Rev. C **75**, 055809 (2007).
[35] R. E. Azuma, E. Uberseder, E. C. Simpson, C. R. Brune, H. Costantini, R. J. de Boer, J. Görres, M. Heil, P. J. LeBlanc, C. Ugalde *et al.*, Phys. Rev. C **81**, 045805 (2010).
[36] N. de Séréville, C. Angulo, A. Coc, N. L. Achouri, E. Casarejos, T. Davinson, P. Descouvemont, P. Figuera, S. Fox, F. Hammache *et al.*, Phys. Rev. C **79**, 015801 (2009).
[37] M. S. Smith, E. J. Lingerfelt, J. P. Scott, C. D. Nesaraja, W. R. Hix, K. Y. Chae, H. Koura, R. A. Meyer, D. W. Bardayan, J. C. Blackmon *et al.*, AIP Conf. Proc. **847**, 470 (2006).
[38] S. Starrfield, J. W. Truran, M. C. Wiescher, and W. M. Sparks, Mon. Not. R. Astron. Soc. **296**, 502 (1998).
[39] R. H. Cyburt, A. M. Amthor, R. Ferguson, Z. Meisel, K. Smith, S. Warren, A. Heger, R. A. Hoffman, T. Rauscher, A. Sakharuk *et al.*, Astrophys. J., Suppl. Ser. **189**, 240 (2010).